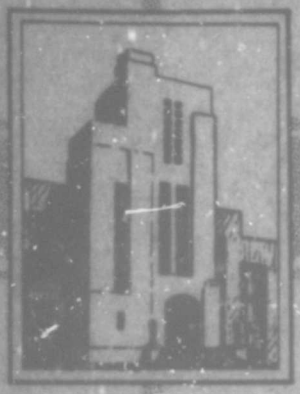

DEPARTMENT OF THE NAVY

DAVID TAYLOR MODEL BASIN

HYDROMECHANICS

AERODYNAMICS

STRUCTURAL MECHANICS

APPLIED MATHEMATICS

AN EXPERIMENTAL INVESTIGATION OF THE STRENGTH OF SMALL-SCALE CONICAL REDUCER SECTIONS BETWEEN CYLINDRICAL SHELLS UNDER EXTERNAL HYDROSTATIC PRESSURE

by

Richard V. Raetz

STRUCTURAL MECHANICS LABORATORY

RESEARCH AND DEVELOPMENT REPORT

March 1960 Report 1397

AN EXPERIMENTAL INVESTIGATION OF THE STRENGTH OF SMALL-SCALE CONICAL REDUCER SECTIONS BETWEEN CYLINDRICAL SHELLS UNDER EXTERNAL HYDROSTATIC PRESSURE

by

Richard V. Raetz

March 1960

Report 1397
S-F013 03 02

TABLE OF CONTENTS

LIST OF FIGURES

LIST OF TABLES

BLANK PAGE

ABSTRACT

Six conical sections, each connecting two cylindrical shells of different diameters, were subjected to external hydrostatic pressure. The cone angle, shell thickness, and cone-cylinder reinforcement were varied to determine their effects on strains and collapse pressures. Good correlation was obtained between calculated and measured strains. Study of the measured and theoretical strains indicated that, for the range investigated, reinforcement at the cone-cylinder junctures should have little effect on the collapse strength of the conical sections. The observed collapse pressures, although affected by fabrication imperfections, lend support to this contention.

INTRODUCTION

At the time conical reducer sections were first used on submarine pressure hulls to connect cylindrical sections of different diameters, a program of study was initiated at the David Taylor Model Basin to determine the structural behavior of these reducers under external hydrostatic pressures. Since basic data on the elastic behavior and collapse strength of truncated steel cones were lacking, three experimental programs on simplified conical sections bounded on one or both ends by cylindrical shells were conducted.

The first series[1] consisted of small conical shells with a rigid closure plate at the small end and a coaxial cylindrical shell at the large end. Strains in the vicinities of the cone-cylinder junctures of these models were measured when they were subjected to *internal* hydrostatic pressure. The validity of various analytical methods for computing strains, some of which were developed at the Model Basin,[2,3,4] was checked with these data.

A second series[5] consisted of six larger models of truncated cones with relatively large thickness-to-diameter ratios and with coaxial cylindrical shells at both ends. These models were subjected to increasing *external* hydrostatic pressure until they collapsed. Half of these models had circumferential reinforcing rings at both cone-cylinder junctures and half did not. Strains at the cone-cylinder junctures were measured for comparison with theory, and the collapse pressures were compiled for a study of the effects of juncture reinforcement and of cone thickness on collapse pressure.

A third series of models is described in this report. These six models were of a similar configuration to those of the second series but were constructed to much smaller scale and had various combinations of cone angles, thicknesses of cone and cylinder plating, and stiffening of the cone-cylinder junctures. The conical shells had larger length-to-thickness and diameter-to-thickness ratios than those of the second series, and were intended to fail in the asymmetric buckling range. The purpose of this last series was to extend the previous

---

[1]References are listed on page 26.

studies of both the elastic behavior and the collapse strength of conical shells to other geometries.

DESCRIPTION OF MODELS

Each model consisted of two cylindrical shells of different diameters joined by a truncated conical shell. Figure 1 is a schematic drawing of a typical model. The geometrical

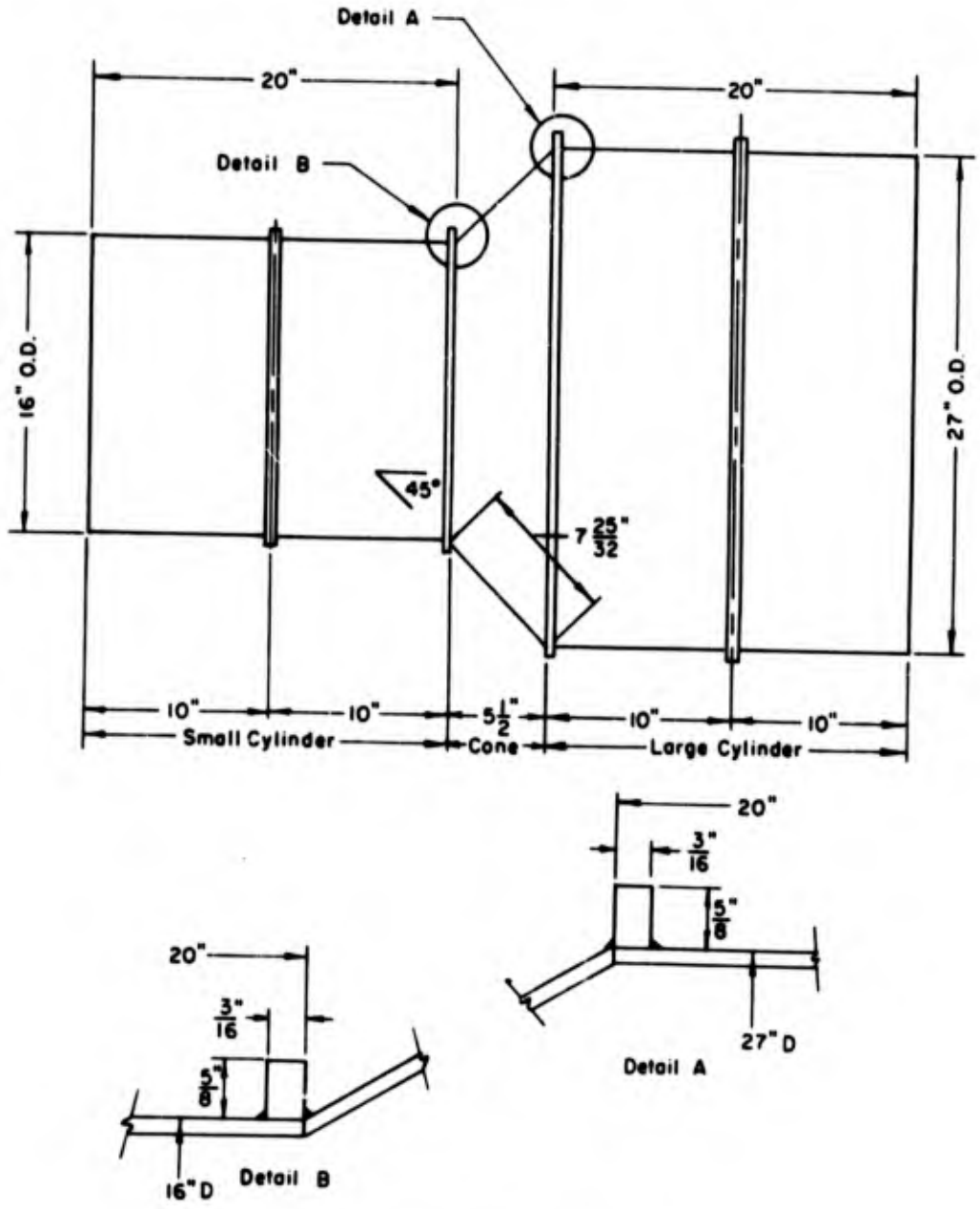

Figure 1 – Schematic Diagram of Model 5

All stiffening rings have same cross-sectional dimensions.

and material properties of the models are given in Table 1. For all models, the large cylinders were of the same diameter and the small cylinders were of the same diameter. Reinforcing rings, wherever used, were the same cross-sectional size, and all models had stiffening rings on the cylinders except Model 1 during its first test.

TABLE 1

Geometrical and Material Properties of Models

Model	Large Cylinder		Cone				Small Cylinder	
	Thickness in.	Yield Point psi	Thickness in.	Yield Point psi	Cone Angle deg	Reinforcement at Cone-Cylinder Juncture	Thickness in.	Yield Point psi
1	0.127	50,000	0.110	42,300	60	At small end	0.092	35,000
2	0.125	50,000	0.110	42,300	60	At both ends	0.092	35,000
3	0.1615	55,300	0.094	65,100	30	At both ends	0.094	65,100
4	0.157	55,700	0.106	66,000	45	None	0.096	64,600
5	0.165	57,600	0.106	66,000	45	At both ends	0.106	66,000
6	0.157	55,700	0.095	63,400	45	None	0.096	64,600

All models were made from sheet steel. Each section was machine-rolled to the correct diameter and welded along a longitudinal seam. The three shell sections were then joined with their longitudinal welds collinear. Before each model was tested, a closure plate was welded to the end of the small cylinder, and a serrated mounting ring, for clamping to the 37-in. pressure test tank, was welded to the large cylinder.

Five models were constructed in this manner. Model 6 was constructed by replacing the conical section of Model 4 after it had failed with one of different thickness.

All longitudinal seams were ground flush with the shell surface except the seam of the cone of Model 6. Circumferential welds were ground flush only at the unreinforced cone-cylinder junctures of Models 1 through 6.

TEST APPARATUS AND PROCEDURE

Wire-resistance strain gages were installed on all models except Model 6. All gage locations were laid out along generators in pairs, one oriented in the longitudinal and one in the circumferential direction. A pair of gages was installed on the external surface at most locations. Gages were also installed on the internal surface of the model at some, but not all, locations. A sample strain-gage location diagram is shown in Figure 2. Model 1 had gages

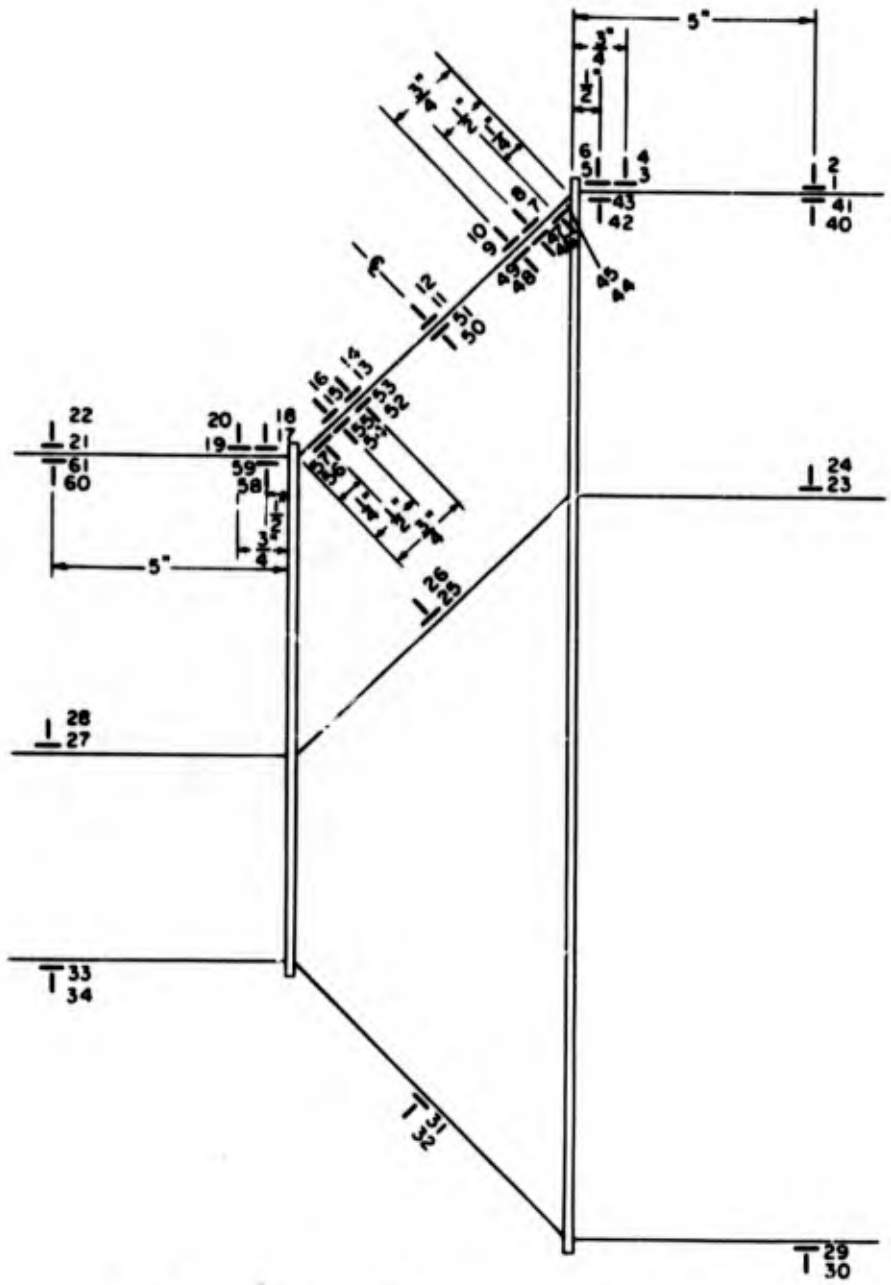

Figure 2 – Gage Location Diagram for Model 5

installed at identical locations along two generators, spaced 90 deg apart, of the cone and cylinders near the junctures. Models 2 through 5 had the same instrumentation as Model 1 along one generator, and some additional gages throughout the length of the cone with some locations being duplicated on two other generators. Models 1 through 5 also had gages installed on the two cylinders far from the intersections to check membrane strains. Strain readings were taken with Baldwin strain indicators.

TABLE 2

Loading Schedule

Model	Run	Pressure Range psi	Data Recorded
1. First test*	1	0- 60	Strains Circularity of cylindrical shells only
	2	0-100	Strains Collapse pressure of large cylinder
1. Second test	1	0- 97	Strains Circularity of cylindrical shells only Collapse pressure of cone
2.	1	0- 80	Strains Circularity
	2	0- 90	Strains Circularity
	3	0-115	Collapse pressure of cone
3.	1	0-105	Strains Circularity Pressure to form first lobe in cone
	2	105-120	Pressure to form second lobe in cone
4.	1	0- 60	Strains Circularity
	2	0-100	Strains Circularity
	3	100-163	Strains, one gage Collapse pressure of cone
5. First test	1	0-100	Strains Circularity
	2	0-100	Strains Circularity
	3	100-135	Collapse pressure of cone
5. Second test	1	0-145	Initial circularity Collapse pressure of cone
6.	1	0-135	Initial circularity Collapse pressure of cone

*The cylindrical shells of all models were reinforced with intermediate stiffening rings after Model 1 failed in the large cylinder during its first test.

Circularities were recorded normal to the surfaces of the shells with an Ames dial gage mounted on an arm which rotated about a shaft coincident with the axis of symmetry of the shells. These records were taken on only the cylinders of Model 1; they were taken at the cone-cylinder junctures and at midlength of the cones of Models 2 through 5. Only the circularity at the midlength of the cone of Model 6 was recorded.

Pressure was applied to the models in the 37-in.-diameter test tank in increments, usually in three runs. The purpose of the first two runs, which were to be taken to a maximum pressure substantially below the expected collapse pressure, was to determine the elastic strain-sensitivity coefficients (microinches per inch per psi) and the circularity patterns under pressure. These measurements were usually taken during the first two runs only. The collapse pressure of the model was determined on the third run. Exceptions to this procedure were the tests of Model 6, the retests of Models 1 and 5, and those cases where the model collapsed prematurely. A loading schedule for all tests is shown in Table 2.

EXPERIMENTAL RESULTS

Models 3, 4, and 5 are shown after collapse, in Figure 3. All plots of strain against pressure, except those for Model 1 during its first test, showed little or no nonlinearity. Some pressure-strain plots of special interest are given in Figures 4 and 5. Strain-sensitivity coefficients for all models are shown graphically in Figures 6 through 10. All strains were measured away from the longitudinal seams. The theoretical strain distributions computed by the methods of Reference 4 are also shown in these figures.

The displacements, normal to the shell surfaces, that were measured during pressure runs were plotted, along with the initial circularities so that displacements normal to the shells could be observed. All displacements were linear with pressure. A typical circularity plot for Model 5 showing displacement under pressure is given in Figure 11.

All failures occurred in a shell-buckling mode. Schematic diagrams of each model tested, with the circumferential orientations of the lobes, gage locations, and longitudinal welds, are shown in Figure 12. All lobes except that in Model 1 during its first test appeared in the conical sections.

The large cylindrical shell of Model 1 buckled near its longitudinal weld at 100 psi. The lobe was straightened out, and circumferential reinforcing rings were installed at midbay in both cylinders. These rings were also used in all subsequent models. During the first run of the retest the conical shell buckled at 97 psi, the lobe extending from 10 to 60 deg from the longitudinal weld. The pressure-strain curves for the first test (Figure 4) become nonlinear at 80 psi, whereas those for the second test remain linear through 90 psi, the highest pressure for which readings were taken.

Model 2 collapsed at 115 psi. The center of the lobe appeared at a point approximately 45 deg from the longitudinal weld. Strains were practically linear with pressure up to 90 psi for all gages.

(Text is continued on page 22.)

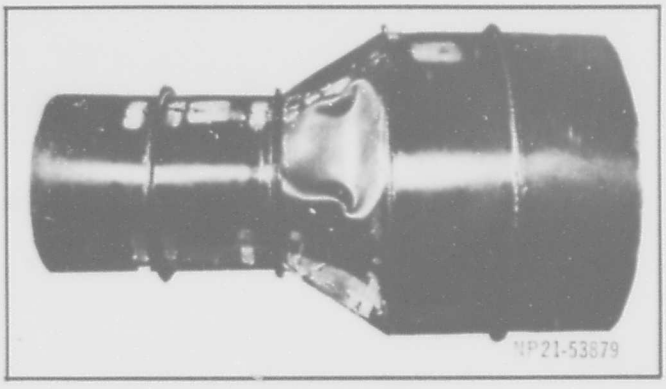

Figure 3a – Model 3

Figure 3b – Model 4

Figure 3c – Model 5

Figure 3 – Photographs of Models 3, 4, and 5 after Collapse

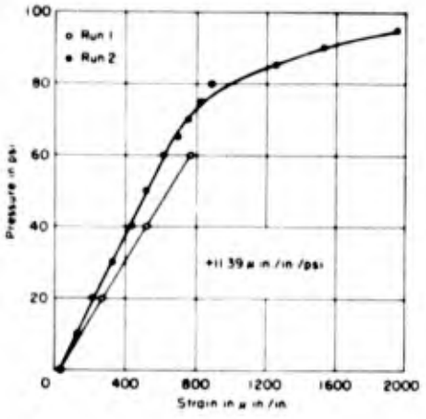

Figure 4a – External Circumferential Strain

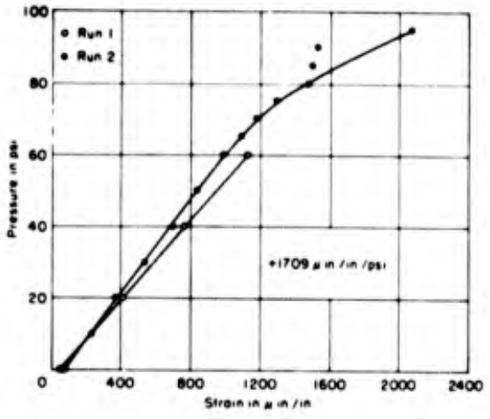

Figure 4b – External Longitudinal Strain

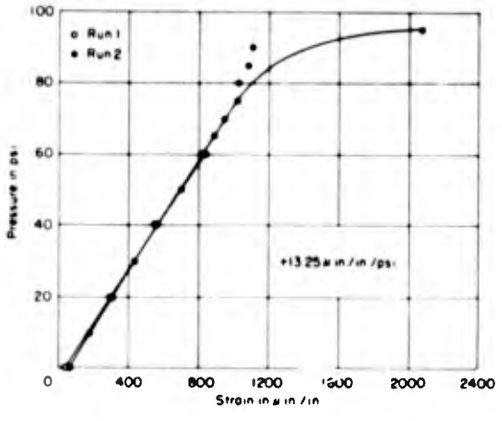

Figure 4c – Internal Circumferential Strain

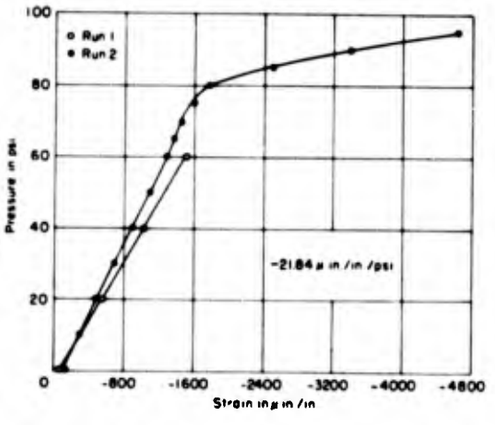

Figure 4d – Internal Longitudinal Strain

Figure 4 – Pressure-Strain Plots for Gages on Cone ¼ Inch from Large Cone-Cylinder Juncture on 90-Degree Generator for First Test, Model 1

The strain-sensitivity coefficient is indicated on each plot.

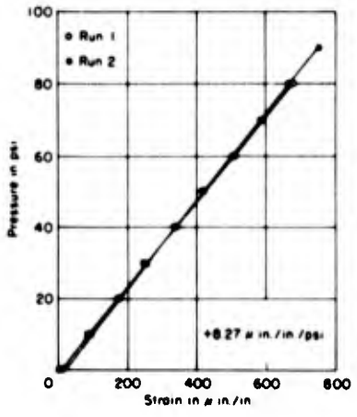

Figure 5a – External Circumferential Strain

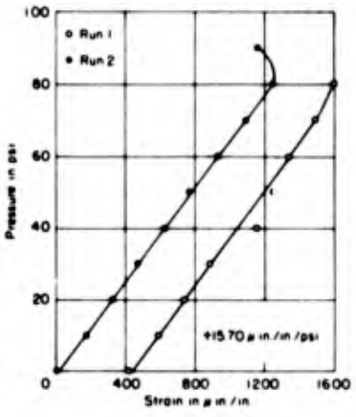

Figure 5b – External Longitudinal Strain

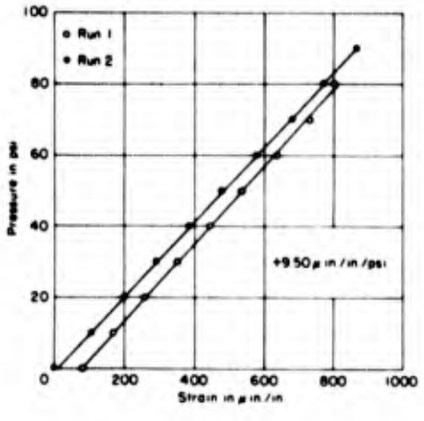

Figure 5c – Internal Circumferential Strain

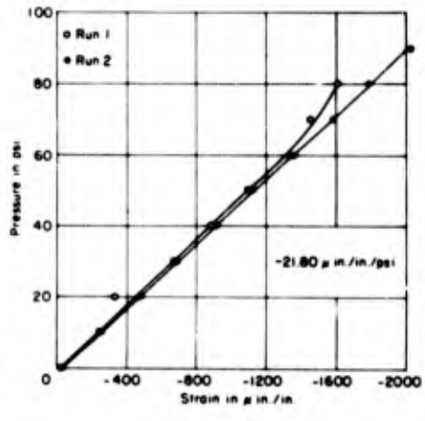

Figure 5d – Internal Longitudinal Strain

Figure 5 – Pressure-Strain Plots for Gages on Cone ¼ Inch from Large Cone-Cylinder Juncture on 0-Degree Generator, Model 2

The strain-sensitivity coefficient is indicated on each plot.

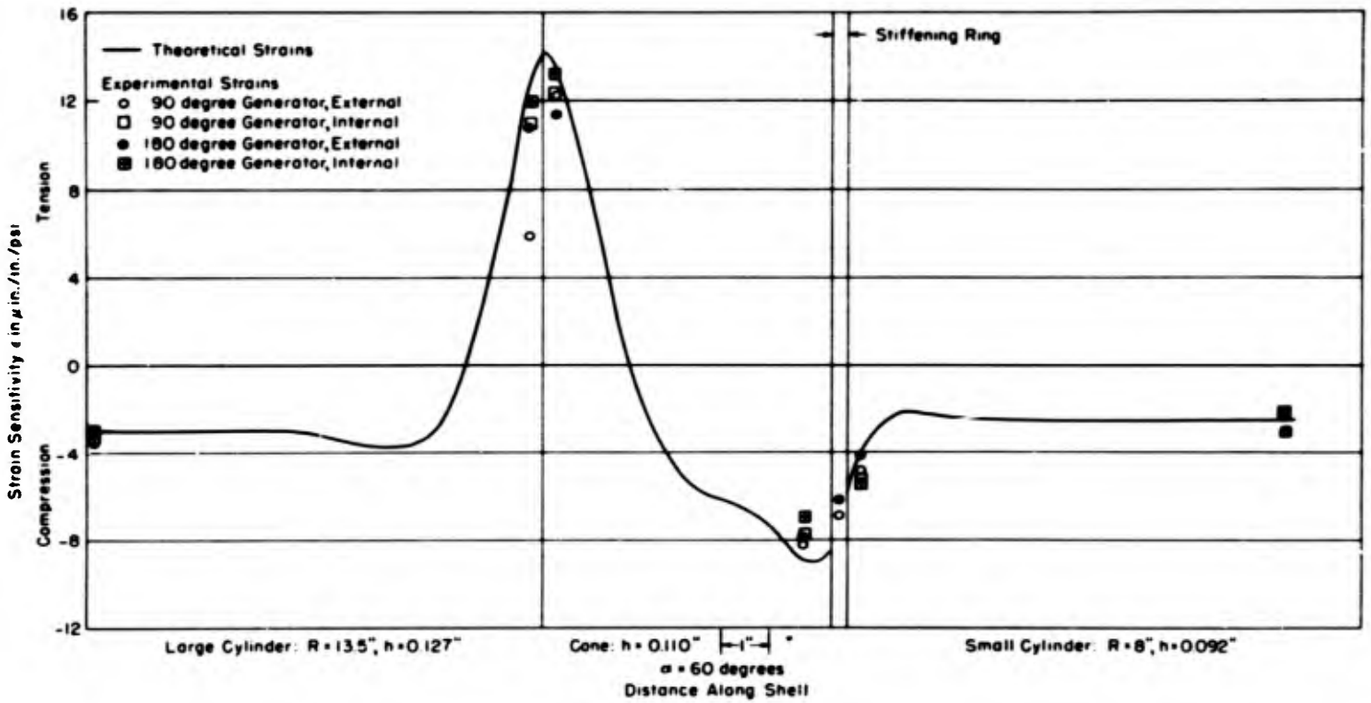

Figure 6a – Circumferential Strains

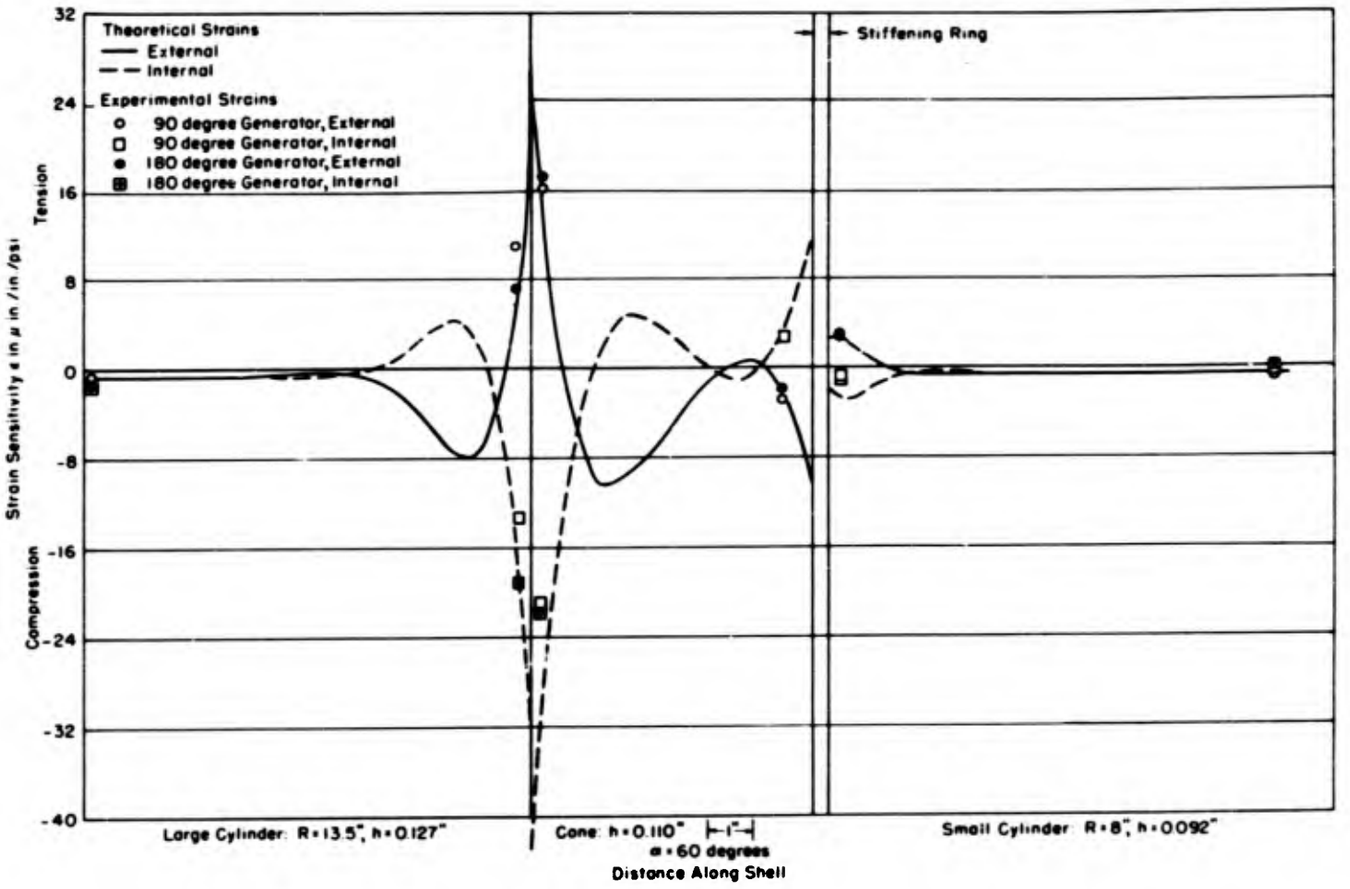

Figure 6b – Longitudinal Strains

Figure 6 – Theoretical and Experimental Strains in Model 1

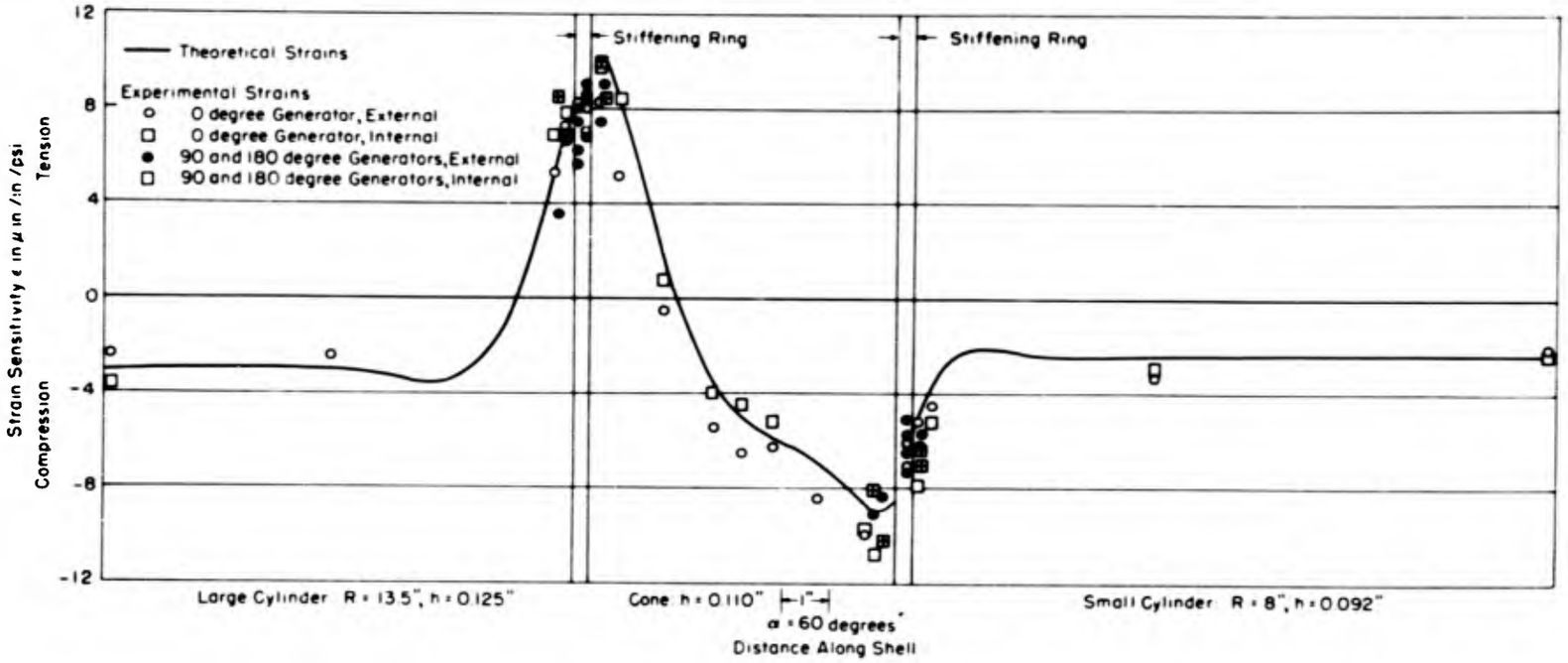

Figure 7a — Circumferential Strains

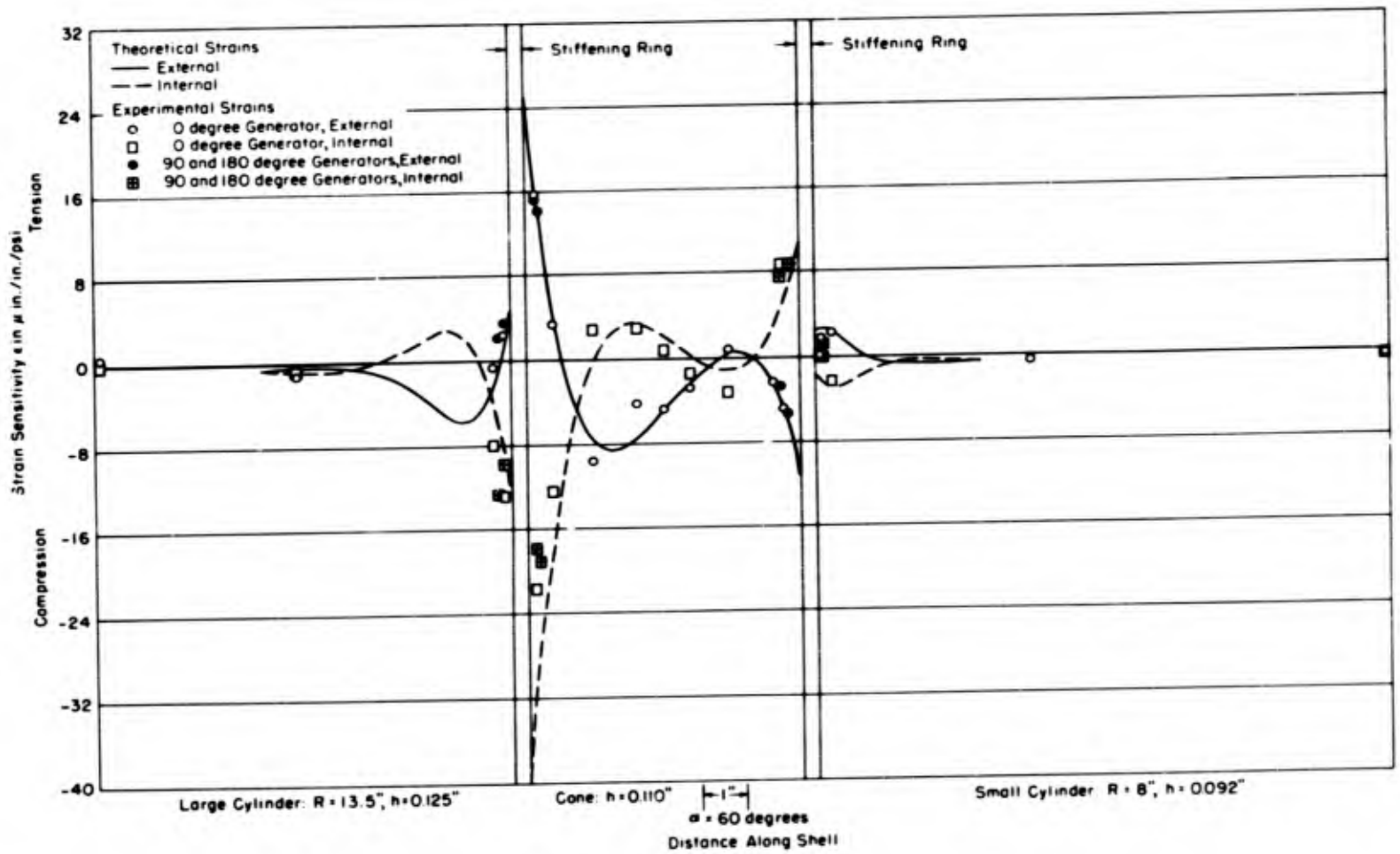

Figure 7b – Longitudinal Strains

Figure 7 – Theoretical and Experimental Strains in Model 2

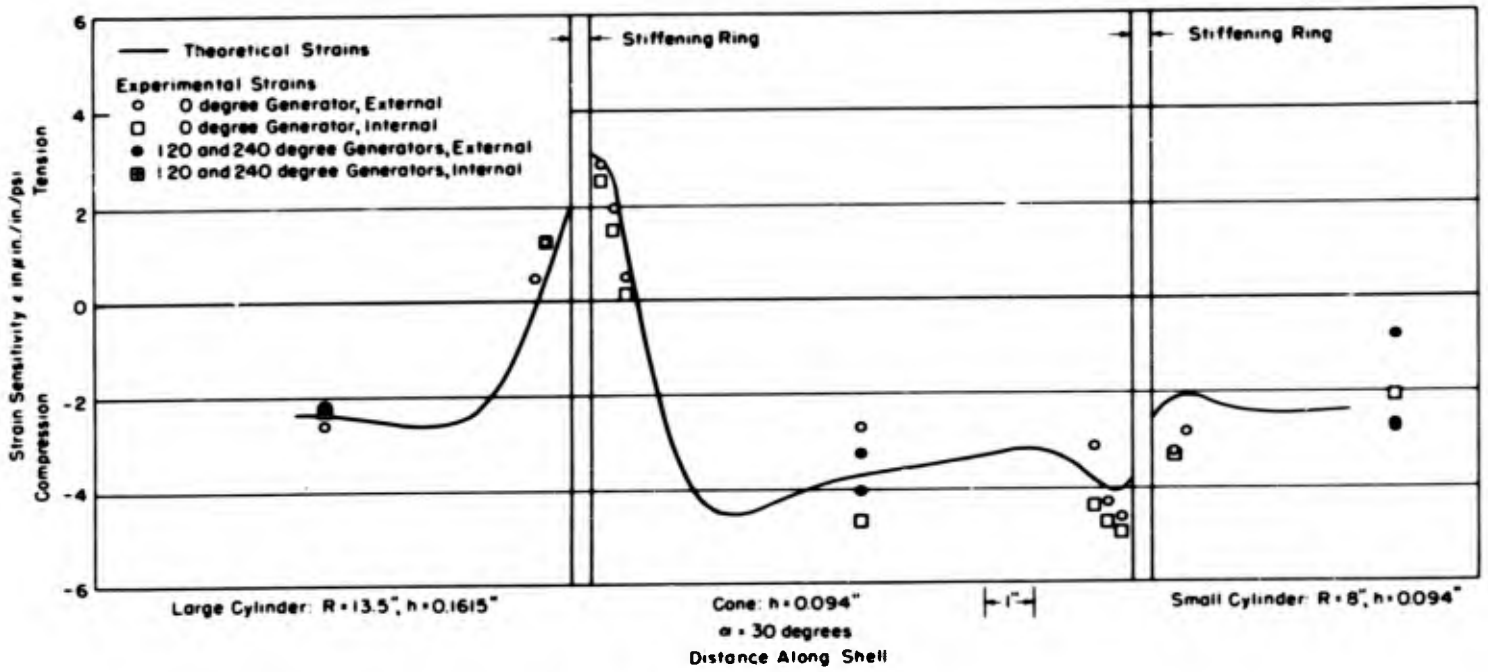

Figure 8a – Circumferential Strains

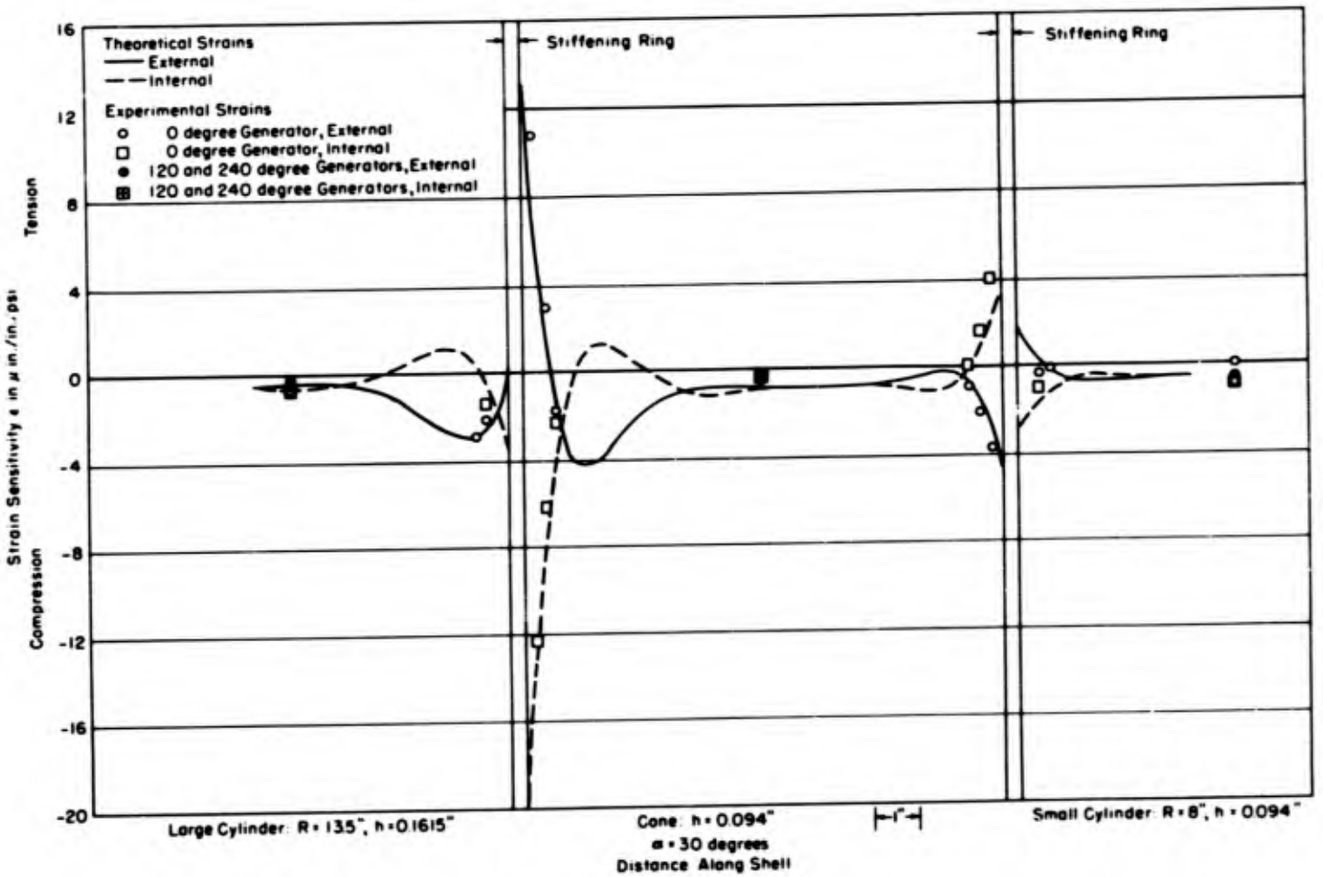

Figure 8b – Longitudinal Strains

Figure 8 – Theoretical and Experimental Strains in Model 3

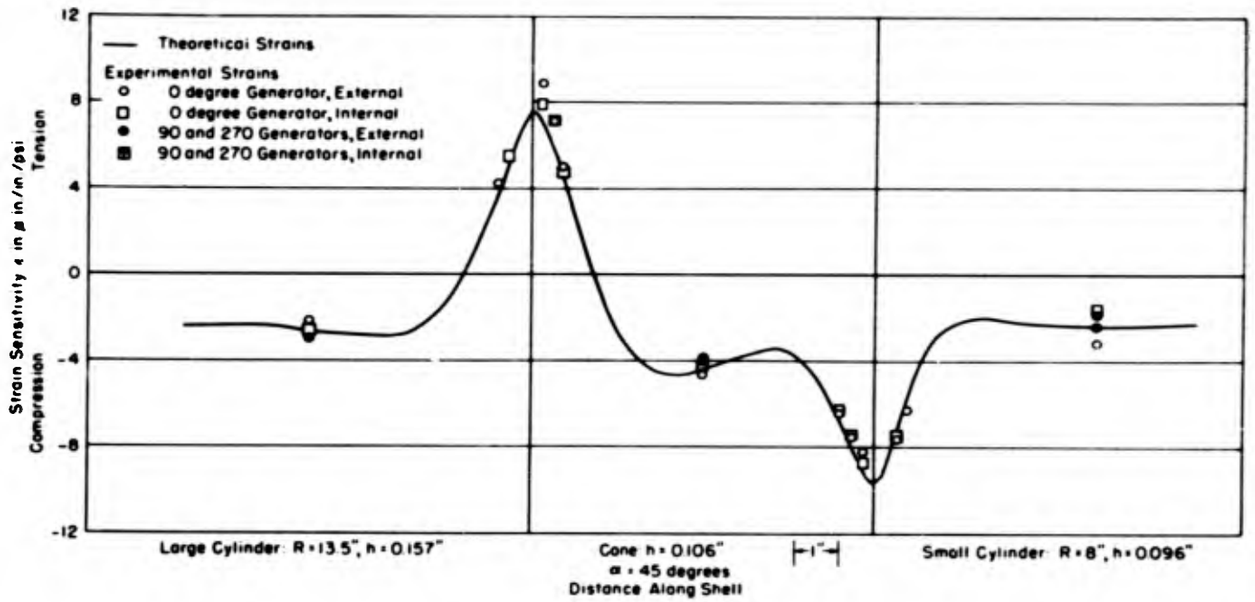

Figure 9a — Circumferential Strains

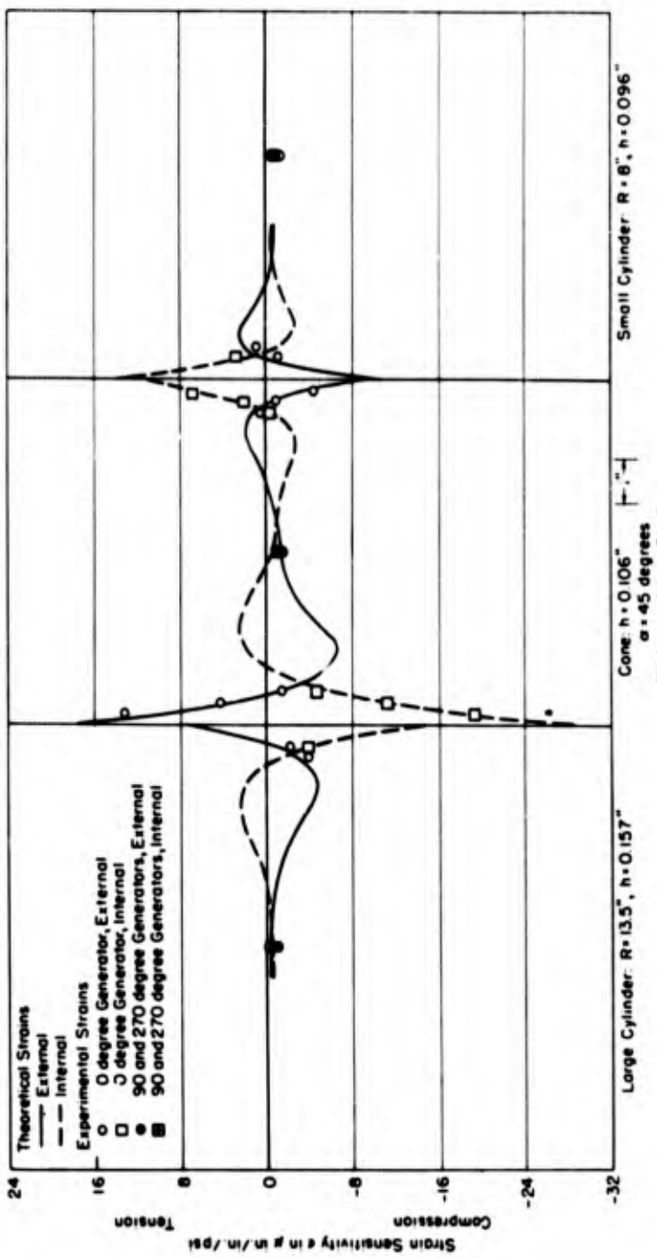

Figure 9b – Longitudinal Strains

Figure 9 – Theoretical and Experimental Strains in Model 4

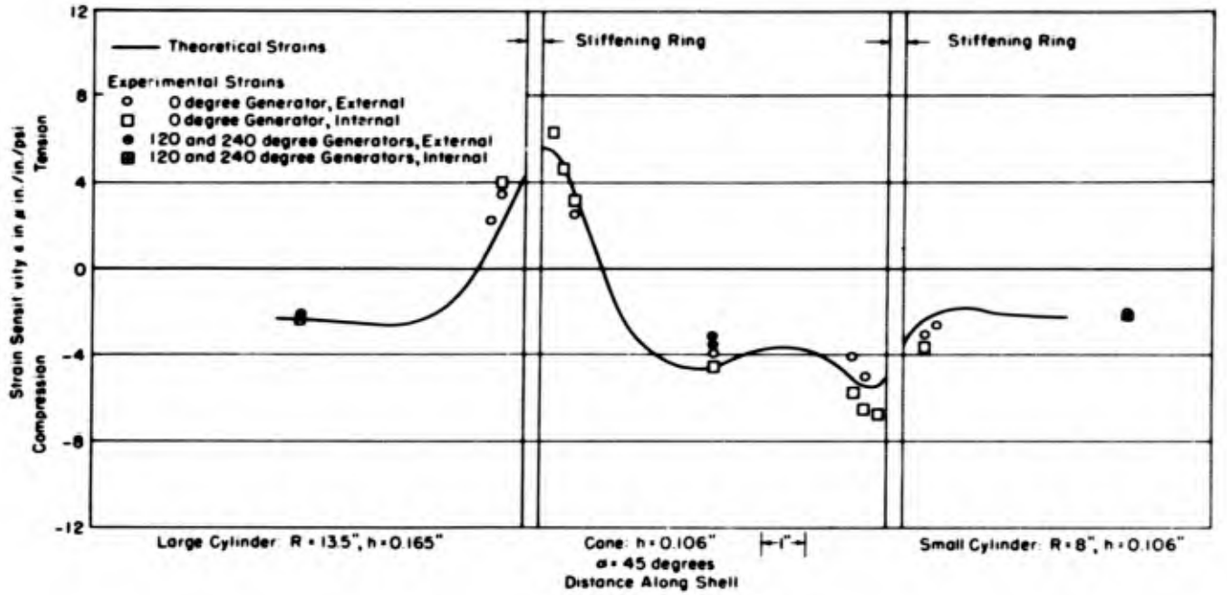

Figure 10a – Circumferential Strains

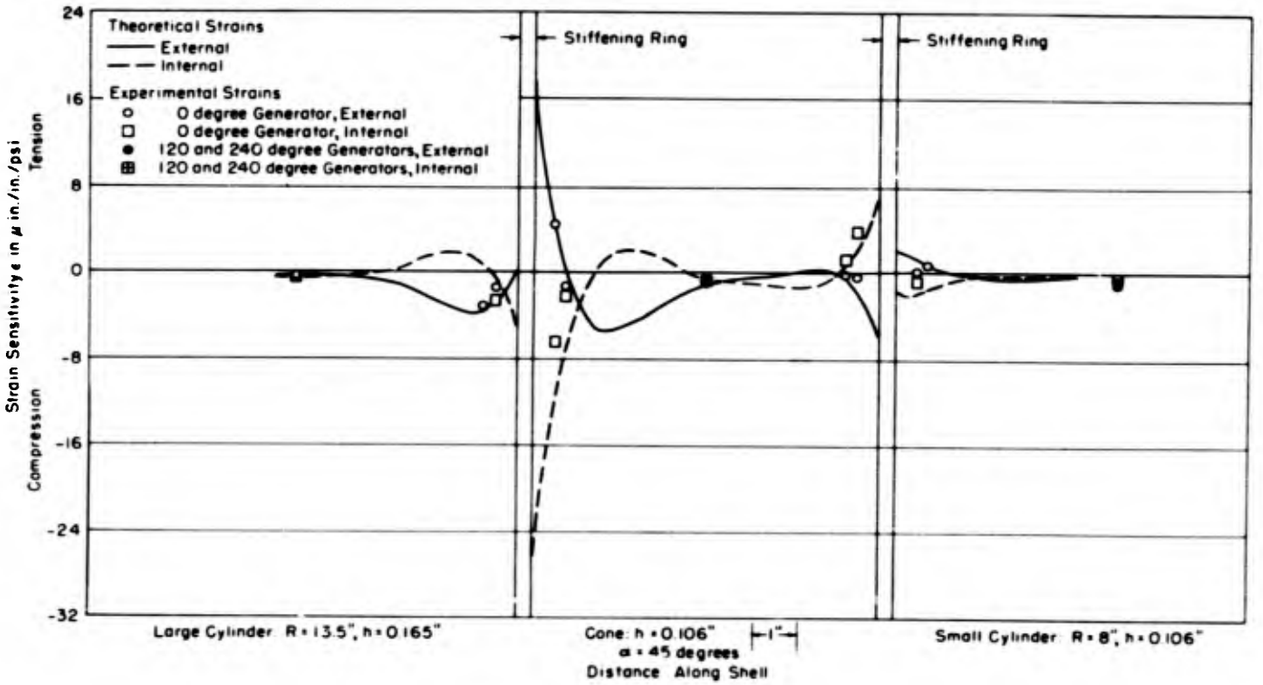

Figure 10b – Longitudinal Strains

Figure 10 – Theoretical and Experimental Strains in Model 5

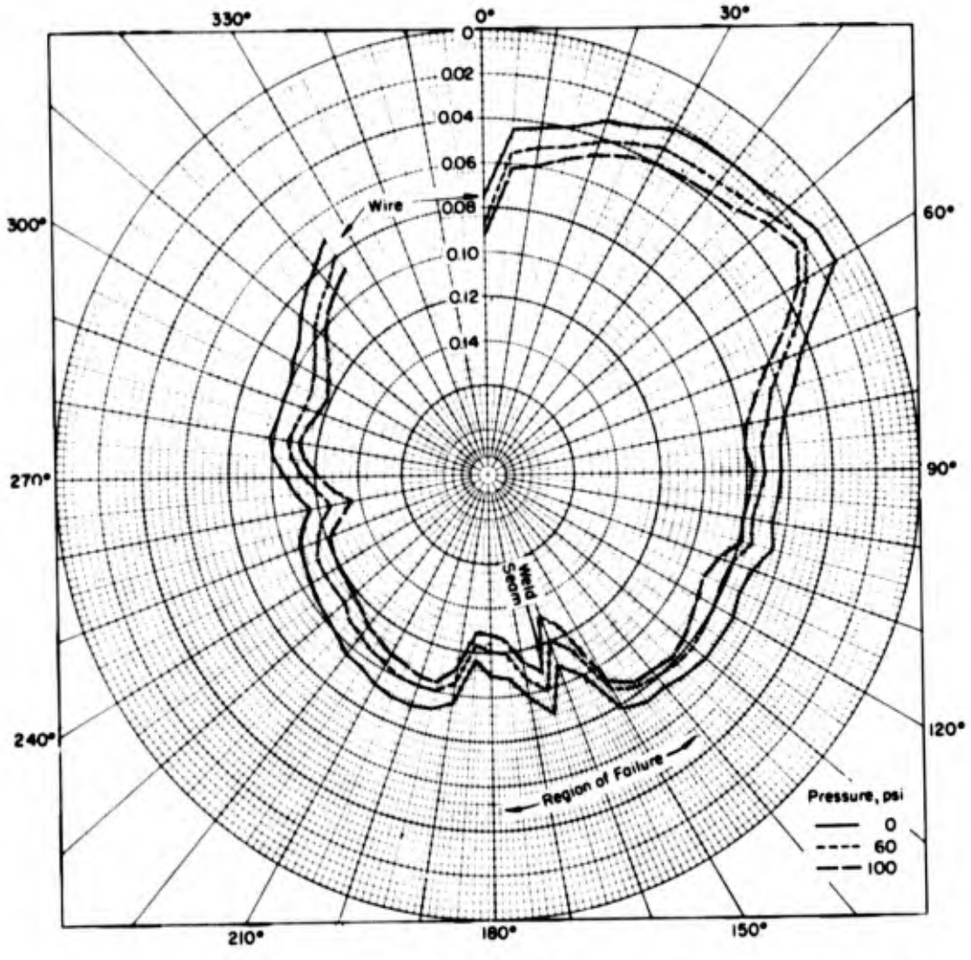

Figure 11 – Radial Deflection of Cone of Model 5 during Run 2 of First Test

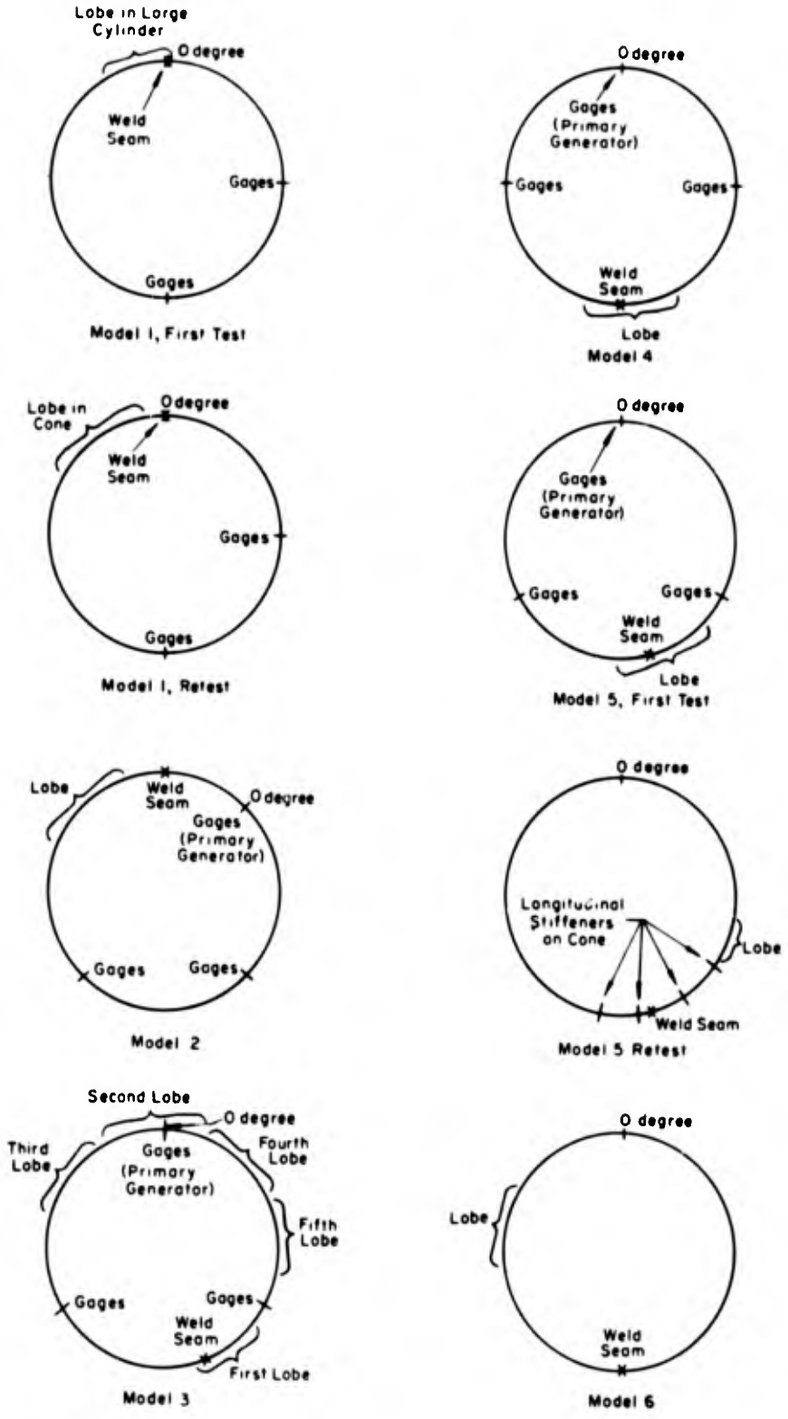

Figure 12 – Schematic Diagram Showing Regions of Failure on Models

All lobes except that in Model 1, Test 1 appeared in the conical sections.

At approximately 80 psi during the first run for Model 3, oil leaks were discovered at the large cone-cylinder juncture by the longitudinal welds and in the weld joining the large cylinder to the serrated mounting ring. Practically no drop in pressure was observed because of the leaks, so the loading was continued until a lobe appeared in the cone at the longitudinal weld at 105 psi. This collapse was attributed to a defective weld, and the pressure was again applied until a second lobe appeared at 120 psi, about 165 deg from the weld. Under continued pumping, three more lobes appeared; the pressure remained below 120 psi.

Model 4 collapsed at 163 psi, with a lobe at the edge of the longitudinal weld in the cone.

Model 5 collapsed at 135 psi. The center of the lobe appeared at the longitudinal weld. Failure was attributed to a weakening influence of the weld, and the model was tested again after the lobe had been straightened out and the area had been reinforced with four longitudinal stiffeners. A lobe appeared during the second test adjacent to the reinforced area at 145 psi. Strains, which were measured during the first test only, were linear with pressure.

The cone of Model 6 was the only shell section in which the longitudinal weld was not ground flush. The model was loaded to the collapse pressure in one run after the initial circularity of the conical shell had been recorded. The first lobe appeared at 135 psi at a point 100 deg from the longitudinal weld.

DISCUSSION

It can be seen from Figures 6 through 10 that, in general, the measured elastic strains agreed well with strains calculated by the methods of Reference 4. These methods represent an approximation which is considered primarily applicable to cones with small vertex angles. Thus the agreement obtained is especially noteworthy for Models 1 and 2, which had large (60-deg) cone angles. The experimental "scatter" shown at almost all gage locations lends evidence that the accuracy of the theory as applied to these models is consistent with the degree of physical perfection of the models (variations in the width of the welds appeared to be on the order of 1/8 in.) and of the testing technique.

Useful comparisons can be made between the strain distributions of Models 1 and 2 (Figures 6 and 7, respectively) and between Models 4 and 5 (Figures 9 and 10, respectively). It can be seen from both comparisons that the reinforcing rings reduced circumferential strains at the large cone-cylinder junctures. Strain distributions for Models 4 and 5 show that both circumferential and longitudinal strains were reduced at the small cone-cylinder junctures by the reinforcing ring. Longitudinal strains in the *conical shells* at the large junctures, however, appeared to be little affected by the rings because the cross sections of the rings rotated in the meridional planes. This rotation is evident from the circumferential strain distributions for Models 2 and 5, and also from the fact that longitudinal strains in the large cylinders of these two models were greatly reduced. Proper design of the juncture to

eliminate the rotation[5] would have made the rings more effective in reducing the maximum longitudinal strains and stresses at the junctures. Theoretical circumferential and longitudinal strains and stresses in the central regions of the conical shells of both pairs of models were almost completely unaffected by reinforcement at the juncture. This was confirmed experimentally by strain measurements in this region on Models 4 and 5.

It is indicated from a study of Figure 12 that the formation of the first lobe during every test except that of Model 6, and possibly that of Model 2, may have been initiated by circumferential yielding in the region of a weld. It may be significant that the longitudinal weld in the conical section of Model 6 was the only one (with the exception of the welds attaching the longitudinal stiffeners to Model 5 for its retest) which was not ground flush with the shell surface. It should be noted that plastic buckling is assumed to be caused by yielding either at the "trough" or at the "crest" point of an embryonic lobe. Thus premature plastic buckling could be caused by yielding in the vicinity of a weld at either the center or the edge of a lobe. It can be seen from Figure 11 that failure of Model 5 occurred in the region of an inward dent which included the longitudinal weld seam. This was observed to be the case, in general, for the other models.

The collapse pressure of the conical section of Model 1 (retest) must be disregarded since it had previously withstood a higher pressure. The collapse pressure during the second test may have been lowered not only by the weakening influence of its longitudinal weld, but also by an increase in out-of-roundness of the conical shell caused by the collapse of the large cylindrical shell during the first test.

Collapse pressures and some pertinent physical and material properties of the models are summarized in Table 3. An important quantity is βl where

$$\beta = \sqrt[4]{\frac{3(1-\nu^2)}{R^2 h^2}}$$

ν is Poisson's ratio,

R is average radius,

h is thickness, and

l is length along the shell between junctures.

βl is the argument of the trigonometric and exponential functions which describe the deflection of the conical shell under pressure. It is shown in Reference 4 that any effect exerted by a discontinuity such as a ring or connecting shell disappears at a distance along the shell of about $3.0/\beta$. Thus the stresses in the midbay region of a shell with a length l of $6/\beta$ or more should be unaffected by adding reinforcement at the edges. This is shown graphically in Figures 6 through 10, in which strain distributions for Models 1 and 2, where $\beta l = 5.45$ are compared with strain distributions Models 4 and 5, where $\beta l = 8.08$. As shown, the strains throughout most of the conical shells are little affected by end conditions. This is consistent also with the results obtained from the second series of tests[5] in which the range of values of

TABLE 3

Summary of Experimental and Calculated Collapse Pressures

	Model					
	1	2	3	4	5	6
Cone angle, deg	60	60	30	45	45	45
Cone thickness, in.	0.110	0.110	0.094	0.106	0.106	0.095
Yield point of cone material, psi	42,300	42,300	65,100	66,000	66,000	63,400
Location of stiffening rings	small end	both ends	both ends	none	both ends	none
Length of cone, in.	6.36	6.36	11.00	7.78	7.78	7.78
βl	5.453	5.453	13.427	8.081	8.081	8.581
Actual collapse pressure, psi	97*	115	105/120**	163	135/148†	135
Calculated collapse pressures, psi						
Tokugawa[6]	237	237	195	334	334	205
Niordson[7]	399 (12)††	399 (12)	146 (10)	290 (11)	290 (11)	220 (11)
Bunich, Paliy, and Piskovitina[8]	202 (8)	202 (8)	161 (8)	237 (8)	237 (8)	179 (9)

*The cone had sustained 100 psi during a previous run, when the large cylinder failed.

**The first lobe appeared at 105 psi in the vicinity of a leaky weld. The second appeared at 120 psi at a point far removed around the circumference.

†The first pressure is that at which the model failed in the vicinity of a suspicious weld. The second was obtained during a retest after the first lobe had been straightened out and the cone had been reinforced with longitudinal stiffeners.

††The numbers in parentheses correspond to the number of lobes at buckling.

βl was from 4.06 to 5.21. There it was found that reinforcement increased the collapse pressure in every case, the increase being higher for models with low values of βl. In the series reported herein, with βl ranging from 5.45 to 13.43, reinforcement at the juncture would not be expected to show much effect on collapse pressure even if no difficulty had been experienced with physical deficiencies of the models.

Some calculated collapse pressures of interest are given in Table 3. In none of these methods are the finite stiffness effects of reinforcing rings at the shell boundaries taken into account. In all these analyses, simple support at the boundaries is assumed and the theories are for elastic buckling. Of the three theories, the most realistic deflection functions appear to have been used in Reference 8. From a consideration of the measured collapse pressure, it is seen that no model sustained its computed elastic buckling pressure. Furthermore, axisymmetric stresses based on experimental and theoretical strain-sensitivity coefficients in the central regions of the conical shells of all models tested are much lower than the yield point of the shell material at the collapse pressures. It seems likely, therefore, that all the

failures occurred in a plastic buckling mode, precipitated by local yielding due to imperfections in the models, out-of-roundness in Models 2 and 6, and a combination of out-of-roundness and weak welds in the others.

CONCLUSIONS

1. The methods of Reference 4 are satisfactory for computing elastic stresses and strains in structures in the range of geometries represented by this series of models.

2. Reinforcing rings at the edges of the conical reducer sections have practically no effect on the stresses throughout most of the shell when the shells are relatively long and thin ($\beta l \geq 6$). In the design of such rings, therefore, only reduction of discontinuity stresses need be considered.

3. Reinforcing rings at cone-cylinder junctures will reduce the maximum stress at the junctures but only if properly designed and placed to control meridional rotation of the rings.

RECOMMENDATIONS

1. An experimental program should be carried out to compare the effect of adding intermediate stiffeners with that of increasing shell thickness on the strength of models within this range of geometries.

2. In future tests of models made from rolled and welded sheet steel sections, especially those of thin material that are to be tested to failure, careful consideration should be given to proper welding practice. It would appear to be a conservative practice not to have the weld seams ground flush with the shell surfaces.

3. Consideration should be given to conducting tests on machined models of conical reducer sections to verify available theories for elastic buckling of these structures, and to developing elastic theory which considers the deflections at the cone boundaries.

4. A theory for computing the plastic buckling pressures of truncated conical shells under external hydrostatic pressure, with or without imperfections, should be developed.

ACKNOWLEDGMENTS

The author wishes to express his appreciation to Messrs. M. F. Borg, H. P. Rietman, and K. P. Arges, who conducted the model tests, and to Messrs. J.G. Pulos and E. E. Johnson, who provided many helpful suggestions in preparing the report.

REFERENCES

1. Borg, M. F., "Observations of Stresses and Strains near Intersection of Conical and Cylindrical Shells," David Taylor Model Basin Report 911 (Mar 1956).

2. Wenk, E., Jr. and Taylor, C. E., "Analysis of Stresses at the Reinforced Intersection of Conical and Cylindrical Shells," David Taylor Model Basin Report 826 (Mar 1953).

3. Taylor, C. E. and Wenk, E., Jr., "Analysis of Stress in the Conical Elements of Shell Structures," David Taylor Model Basin Report 981 (May 1956).

4. Raetz, R. V. and Pulos, J. G., "A Procedure for Computing Stresses in a Conical Shell near Ring Stiffeners or Reinforced Intersections," David Taylor Model Basin Report 1015 (Apr 1958).

5. Krenzke, M. A., "Hydrostatic Tests of Conical Reducers between Cylinders with and without Stiffeners at the Cone-Cylinder Junctures," David Taylor Model Basin Report 1187 (Feb 1959).

6. Tokugawa, T., "An Approximate Method for Calculating the Collapse Pressure of Thin Cylindrical, Conical, and Spherical Shells under Uniform External Pressure." Report read at a lecture meeting of the Zōsen Kyōkai (Shipbuilding Association) held Nov 17, 1940.

7. Niordson, F. I. N., "Buckling of Conical Shells Subjected to Uniform External Lateral Pressure," Transactions of the Royal Institute of Technology, No. 10 (1947).

8. Bunich, L. M., et al., "Stability of a Truncated Conical Shell under the Action of Uniform External Pressure," Research and Advanced Development Division, Avco Manufacturing Corporation Report (1958). Translation from the Russian by M.I. Yarymovych, Columbia University.